

NUMERICAL MODELING OF THREE-DIMENSIONAL VENTILATION DUCT FLOW

N. Jovicic¹, D. Milovanovic¹, M. Babic¹, J.V. Soulis²

¹ Faculty of Mechanical Engineering, University of Kragujevac, Yugoslavia

² Democriton University of Thrace, Department of Civil Engineering, Xanthi, Greece

ABSTRACT

Presented in the paper is an efficient and accurate numerical method for simulation of ventilation duct flow. The mathematical method is based on the three-dimensional incompressible RANS equations with isotropic $k-\omega$ near-wall turbulence closures, written in generalized curvilinear coordinates in strong conservation form. The numerical method presented here is used to calculate the turbulent flow through a bend of rectangular ventilation duct featuring pressure induced secondary motions and rotation effects on turbulence. The problem has been the subject of an experimental study of Kim and Patel (1994). Numerical results are compared with experimental data.

KEYWORDS

Ventilation duct, three-dimensional flow, CFD, RANS, turbulence models

INTRODUCTION

Understanding of flow field details is crucial for designing of high efficiency ventilation systems. In order to achieve low energy loss, as well as low noise numerical simulation could be very attractive at an early stage in a project. From an engineer's point of view, the RANS equations in conjunction with two-equation turbulence models is an optimal choice for a reliable prediction of high Re turbulent flow through complex domains. In order to resolve phenomena in near-wall regions, numerical simulations require a very large number of grid points and extremely small grid spacing. Such meshes can dramatically deteriorate the convergence rate of numerical procedure. In order to make accurate, efficient and low-cost code for engineering purposes, it is necessary to apply the appropriate acceleration techniques. Among them, the multigrid method is the most efficient technique known today (Hirsch 1988). Objective of this paper is to present a numerical method for the analysis of 3D incompressible internal flows. The numerical procedure is based on the multistage Runge-Kutta scheme, proposed by Jameson et al., (1981), in conjunction with local time stepping, implicit residual smoothing and the multigrid method. In order to demonstrate the applicability of our numerical tool, it is applied to calculate a turbulent flow through a square sectioned 90 degree bend, for which Kim and Patel (1994) have provided detailed experimental data. Deng et al., (1997) and Sotiropoulos et al., (1998) performed calculations on a curved duct turbulent flow calculations based on the numerical solution of the RANS equation. Deng et al., (1997), used two original near-wall Reynolds-stress

transport models and very fine grid (480000 grid points). Sotiropoulos et al., (1998) performed computations on a slightly coarser-grid (350000 grid point) using two nonlinear variants of $k-\omega$ model based on the quadratic and cubic constitutive relations. We present numerical results obtained using a practical, coarser grid (202000 grid points), which corresponds to computing resources that are typical of those available to an industrial engineer, placing more grid points near the passage walls.

NUMERICAL METHOD

The three-dimensional incompressible RANS equations with isotropic two-equation, near-wall turbulence closures, are written in generalized curvilinear coordinates in strong conservation form (Soulis et al., 1998). The $k-\omega$ model (Wilcox, 1994) is chosen because it is the only available closure without restrictions on the distance from the wall to the near-wall grid point, which is very appropriate for complex geometrical configurations.

The artificial compressibility method is employed to couple the velocity and pressure field in the mean flow equations. The governing equations are discretized on a collocated mesh using the cell vertex finite volume method. The convective fluxes in RANS equation are discretized using second-order central-differencing in conjunction with a flux difference splitting upwind third-order accuracy scheme (Rogers&Kwak, 1988). Three-point central differencing is employed for the viscous fluxes and source terms in turbulence closure equations. The convective flux of turbulence closure equations is formed using Roe's upwind scheme (Hirsch, 1988) with monotone (TVD) interpolation at the cell face (Zijlema,1996).

The discrete mean flow and turbulence closure equations are advanced in time using a pointwise implicit (Zheng et al., 1997) four-stage Runge-Kutta scheme enhanced with local time stepping, variable coefficients implicit residual smoothing and multigrid acceleration. For most two-equation models, the source terms are usually dominant and become stiff near the solid wall and the efficiency of solution then totally depends on the treatment of those source terms. In our numerical model, the source terms in the k and ω equations are divided into two groups locally according to their sign and then only negative parts are treated implicitly. This so-called point-implicit technique is employed to improve the efficiency of the solution and to alleviate the stiffness of the governing equations in the near-wall region. In the present paper the local time step limit is computed with scaled spectral radii of the flux Jacobian matrices for the convective terms. A variable coefficients implicit residual smoothing is used to extend the stability limit and robustness of the basic scheme. The variable coefficients depend on the spectral radii of the flux Jacobian matrices as well as Courant numbers of the smoothed and unsmoothed scheme. A time-lagged or loosely-coupled approach is employed in solving the Navier-Stokes equations and two equation turbulence model in a time marching method, i.e., mean flow and turbulence closure equations are solved separately. A three level V-cycle multigrid algorithm with semi-coarsening in the transverse plane is applied only to the mean flow equations with one, two and three iterations performed on the first, second and third grid level, respectively. The turbulence closure equations are solved only on the finest mesh and eddy viscosity is injected to the coarser meshes and kept frozen during the multigrid process. Three single-grid iterations are performed on the turbulence closure equations per multigrid cycle (Lin et al., 1997).

APPLICATION

Kim and Patel (1994) provided detailed experimental data of the development of turbulent air flow with constant temperature through a 90 deg bend with rectangular cross-section. The duct geometry and the locations of the measured stations are shown in Fig. 1. The bend section was connected to straight inlet and outlet tangents, all of rectangular section $6H \times 1H = 121.8 \times 20.3$ mm. Inlet bulk axial velocity corresponds to a fully developed turbulent flow in a rectangle section duct was $U_0 = 16$ m/s. Reynolds number based on the bulk axial velocity and hydraulic diameter was $Re = 2.24 \cdot 10^5$.

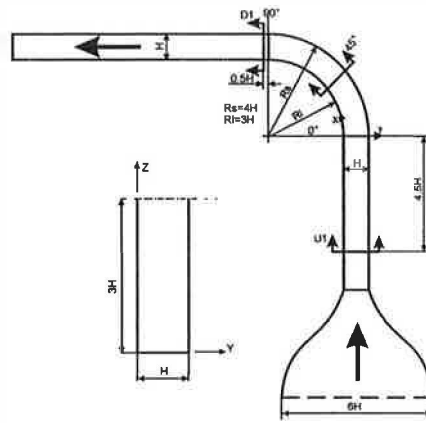


Fig. 1 Flow geometry and coordinate system used

The computational domain starts $4.5H$ upstream from the inlet of the bend (station U1) and extends up to $30H$ downstream from the exit of the bend. Due to flow field symmetry, only half of the domain is considered. Domain is discretized by 202581 grid points ($81 \times 41 \times 61$). For inflow conditions the measurement data at location U1 are used. Due to space limitations, only a sample of the computed results is compared with the experimental data at three station, using four Z -cons. lines (Fig. 2 - 4).

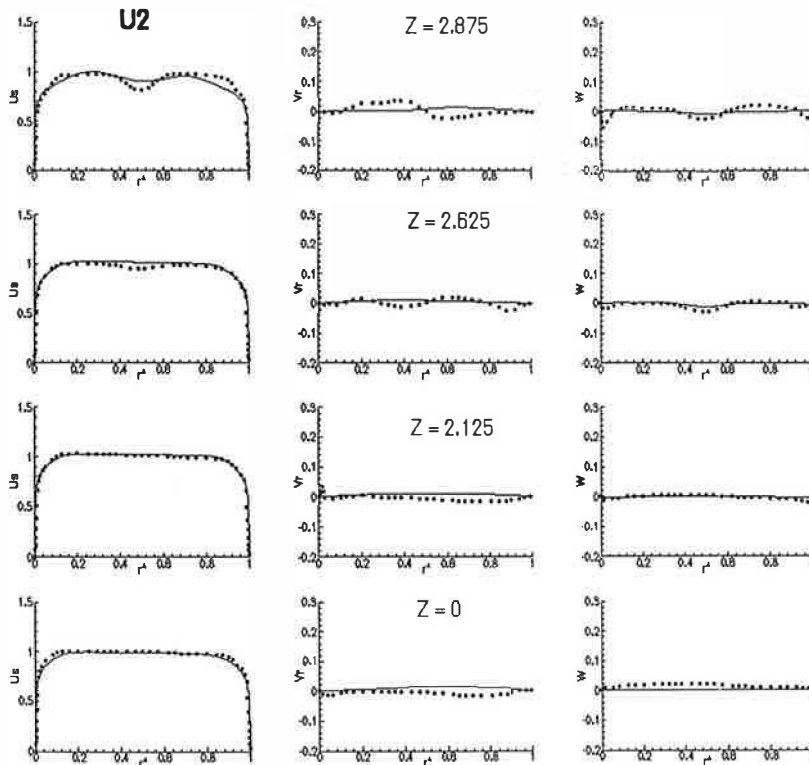


Fig. 2 Measured (Kim & Patel, 1994) and computed velocity profiles at U2 position.

At the station U2 (Fig. 2) the experimental results, as well as numerical results show distortion of streamwise velocity profile due to the inlet contraction-induced vortex pair. This is especially visible near the center of bottom wall.

The measured velocity profiles near the center of the bottom wall at 45 deg. (Fig. 3) are still distorted because the contraction-induced vortex pair continues to affect the flow within the bend. The favorable pressure gradient along the inner wall accelerates the flow and causes the maximum of the axial velocity profile to be shifted from the center toward the inner wall of the bend. The transverse pressure gradient, on the other hand, gives rise to significant secondary motion (sharp peak of the W profiles near the inner wall). This pressure-driven secondary motion acts to reduce the mean streamwise velocity near the inner wall by transporting there low-momentum fluid from the bottom wall boundary layer (U-velocity profile at $Z = 2.875$).

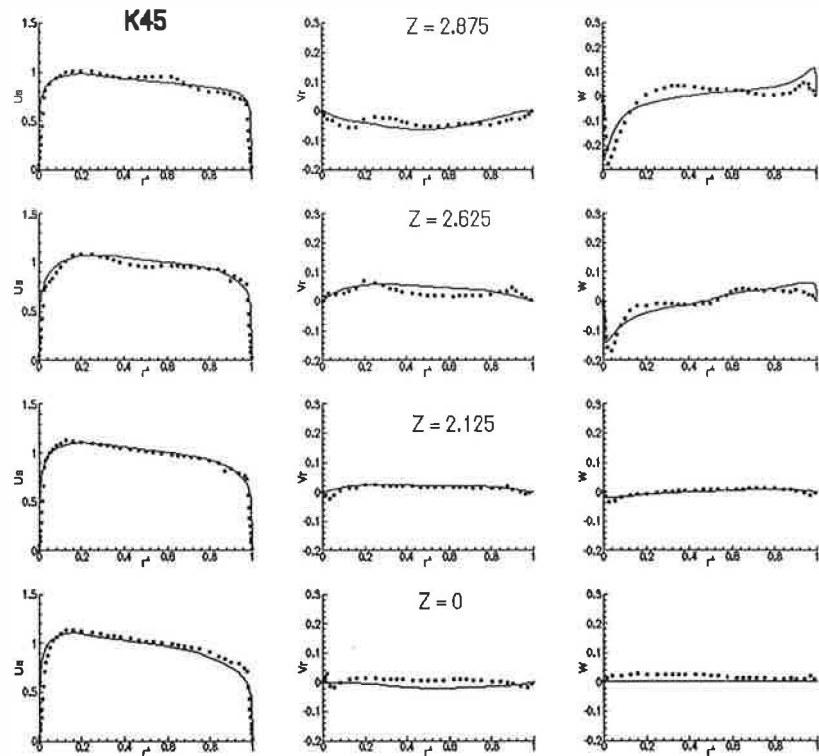


Fig. 3 Measured (Kim & Patel, 1994) and computed velocity profiles at 45 deg.

Unlike at 45 deg position (K45), the opposite pressure gradient at D1 position (Fig. 4) causes the flow acceleration near to the outer wall.

The pressure distribution along the channel at different $r = \text{cons.}$ and $z = \text{cons.}$ location is shown in Fig. 5. The pressure gradient induced by the curvature can be clearly seen. On the convex side, the boundary layer is subjected to a favorable pressure gradient starting upstream of the bend, and this is followed by an adverse gradient around the bend exit. The boundary layer on the concave side is subjected to pressure gradients of similar magnitude but opposite signs. Pressure distribution in the bend is visualized in Fig. 6.

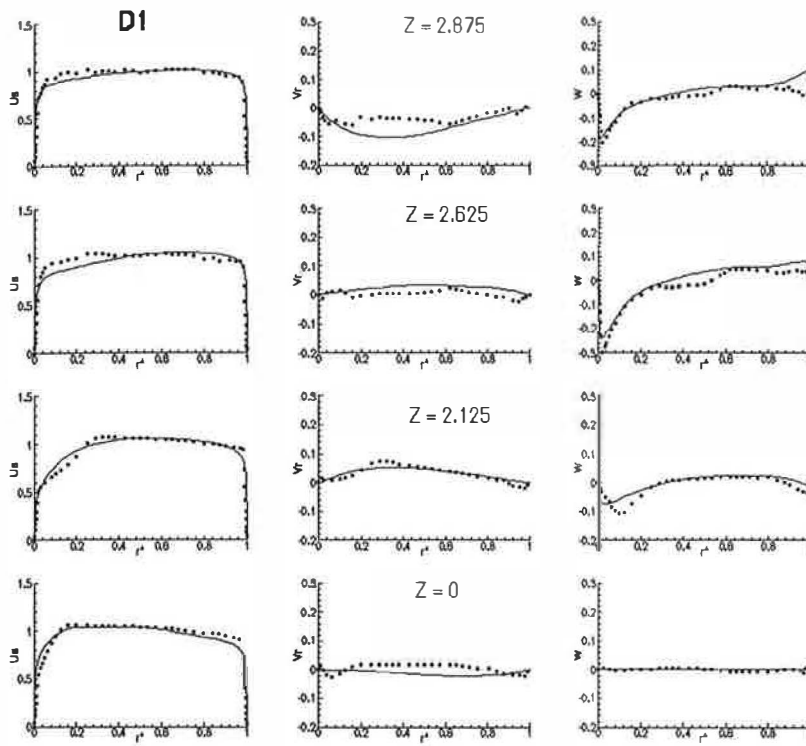


Fig. 4 Measured (Kim & Patel, 1994) and computed velocity profiles at D1 position.

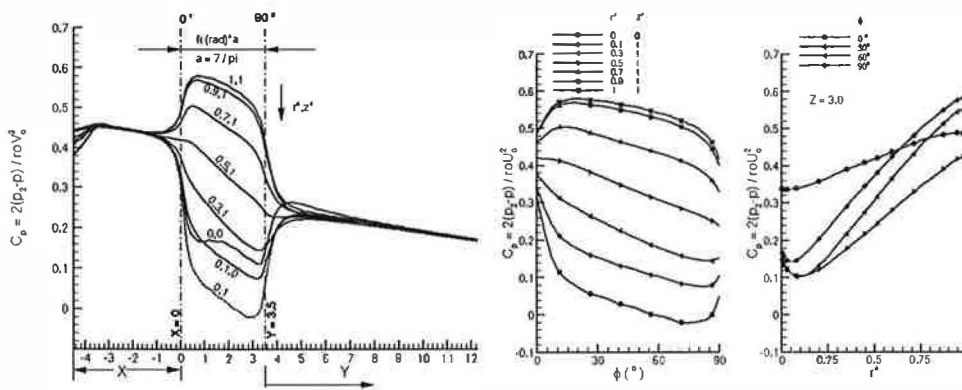


Fig. 5 Computed pressure coefficient distribution along the channel

CONCLUSION

The results obtained using numerical model based on RANS equation with isotropic two-equation near-wall turbulence model, show that global features of the flow field are correctly resolved but some significant differences between measured and numerical results still remain. The same is noticed in

Sotiropoulos et al., (1998) even in case a non-linear near wall turbulence closure is employed. A key factor in obtaining the correct primary flow is the secondary motion prediction with reasonable fidelity.

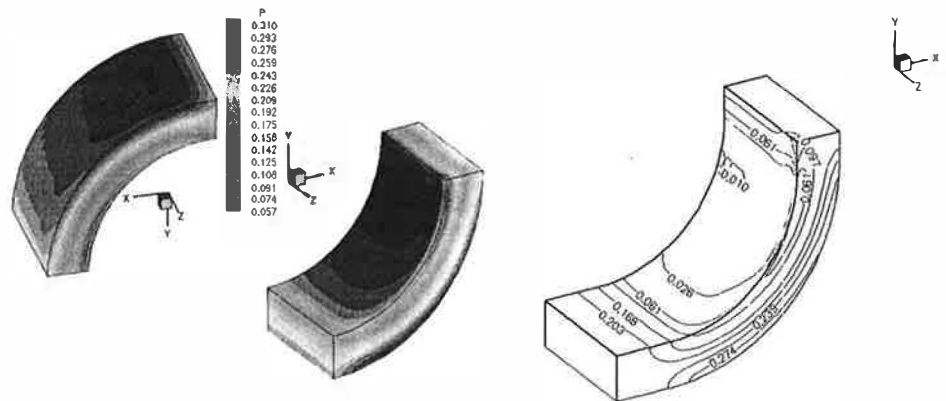


Fig. 6 Computed pressure distribution in the bend

Some differences between measured and computed values are, probably, due to failure of the isotropic two-equation turbulence model to resolve the turbulence structure in a bend that is significantly influenced by its curvature. The general conclusion is that the presented method needs some further improvement to resolve some subtle details that are not fully captured by the method.

REFERENCES

- Deng G.B, Visonneau M. (1997), Assessment of Second-Moment Turbulence Closures for Three-Dimensional Vortical Flows, *ASME FEDSM97*-3169.
- Hirsch C. (1988). *Numerical Computation of Internal and External Flows, Volume 2: Computational Methods for Inviscid and Viscous Flows*, John Wiley & Sons.
- Kim W. J, Patel V. C. (1994), Origin and Decay of Longitudinal Vortices in Developing Flow in a Curved Rectangular Duct, *Journal of Fluid Eng.*, **116**, 45-52.
- Lin F.B. and Sotiropoulos F. (1997). Strongly-Coupled Multigrid Method for 3-D Incompressible Flows Using Near-Wall Turbulence Closures, *Journal of Fluid Eng.*, **119**, 314-324.
- Rogers, S E, Kwak D. (1988), An Upwind Differencing Scheme for the Steady-State Incompressible Navier Stokes Equations, *NASA TM* 101051.
- Sotiropoulos F., Ventikos Y., (1998), Prediction of Flow 90-Degree Bend Using Linear and Nonlinear Two-Equation Turbulence Models, *AIAA Journal*, **36:7**, p. 7.
- Wilcox D. (1994). Simulation of Transition with a two-equation turbulence model, *AIAA Journal*, **32:2**, p.285.
- Zijlema M. (1996). Computational modeling of turbulent flow in general domains, *Ph.D Thesis*, Delft University of Technology, Netherlands.
- Zheng, S, Liao, C, Liu, C, Sung, C H, Huang, T T. (1997). Multigrid Computation of Incompressible Flows Using Two-Equations Turbulence Models, *Journal of Fluids Eng.*, Vol. 119, pp. 893-899.6.
- Jameson, A, Schmidt, W, Turkel, E. (1981). Numerical Solutions of the Euler Equations by Finite Volume Methods Using Runge-Kutta Time Stepping Schemes, *AIAA paper* No. 81 - 1259.
- Soulis, J V, Jovicic, N, Milovanovic, D, et al (1998). Numerical Modeling of Incompressible Turbulent Flow in Turbomachinery, *Computational Fluid Dynamics '98* edited by Papailiou, K., et al., pp. 259-265, John Wiley&Sons.